Melt Shear Rheology and pVT Behavior of Polypropylene / Multi-Walled Carbon Nanotube Composites

NICOLETA VIOLETA STANCIU*, FELICIA STAN, CATALIN FETECAU
Center of Excellence Polymer Processing, Dunarea de Jos University of Galati, 47 Domneasca, 800008 Galati, Romania

In this study, capillary rheological tests were performed on polypropylene filled with multi-walled carbon nanotubes (PP/MWCNT) to determine the melt flow curves and pressure-Volume-Temperature (pVT) diagrams. Based on the experimental data, master viscosity curves were constructed using the time-temperature-superposition principle and the Cross and Carreau-Winter models, while the pVT data were fitted to the Tait equation in both liquid and solid states. Results show that the melt shear viscosity decreases with increasing melt temperature and shear rate and increases with MWCNT wt.%. All composites display shear-thinning behavior in the range of medium to high shear rates. The specific volume of PP/MWCNT composite decreases with increasing MWCNT wt.% and pressure and increases with increasing temperature.

Keywords: carbon nanotubes, polypropylene, melt shear viscosity, pVT measurement

Carbon nanotubes (CNTs) are considered an ideal reinforcement to improve mechanical and electrical properties of polymers, due to their outstanding properties such as high elastic modulus and strength, high electrical and thermal conductivity, high water and chemical resistance [1-5]. In general, scientific literature results provide extensive information on both mechanical and electrical properties of polymer/CNT composites [1-11]. However, little research has yet been conducted on the rheological [7-18] and pVT behaviors [7] of polymer/CNT composites despite the fact that these data are very important for melt processing of these composites [7, 19-25].

Usually, the addition of fillers increases the melt viscosity of the polymers leading to changes in the processing parameters as compared to unfilled polymers [7-18, 26-29]. However, changing the processing parameters is not always easy to control, as it may alter the manufacturing technologies, which invariably involves financial penalty. On the other hand, CNTs give rise to less die swell and shrinkage due to decreased melt elasticity [17], which is an important advantage for polymer/CNT composite manufacturing. The polymer shrinkage during the injection cycle is one of the factors that determine the molding quality [23, 24]. The volumetric shrinkage of the molded part can be predicted based on the volumetric change of the polymer as it cools down from the molten state to the solid state. Thus, to predict the shrinkage a pVT diagram should be considered.

In the light of the large volume of polymers and polymer/CNT composites being processed by melt processes, the polymer manufacturing industry takes advantages of simulation technologies, which can enhance the fabrication by providing quick and accurate assessments of different aspects before the part and mold are built, e.g. how the polymer fills into the mold and cools during the injection molding process, optimization of processing conditions (temperature, pressure, flow rate and duration of flow) etc [25]. However, the accuracy of the simulation results depends on the accuracy of the input material data, such as rheological, thermal, and pVT data, and mechanical properties. Since limited experimental data are available on the rheological models [7-18] and pVT diagrams [7] for polymer/CNT composites, simulations are based on the experience with unfilled polymers. Thus, in this paper, melt shear rheological tests were carried out to determine the melt flow curves and pVT diagrams of polypropylene filled with multi-walled carbon nanotubes and extract the material parameters for modeling of manufacturing processes, such as extrusion or injection molding.

Experimental part

Materials

Polypropylene is one of the most used polymers in the world, but it is not typically used in industry without some modifications such as fillers. The presence of fillers usually increases the melt viscosity, which can have a large impact on the melt processability [18]. Thus the material investigated in this paper is a commercial available polypropylene filled with 1, 3 and 5 wt.% of multi-wall carbon nanotubes (MWCNTs) supplied by Nanocyl (Sambreville, Belgium). Thin MWCNTs with an average diameter of 9.5 nm and length of 1.5μm (type Nanocyl™ NC7000) produced by catalytic carbon vapor decomposition (CCV) method were incorporated into the PP matrix by melt mixing. The temperature of the melt was set at 235-240°C [30, 31]. These PP/MWCNT composites have been previously characterized by calorimetry and other techniques [11, 31].

Characterization

Melt Shear Rheological Measurements

Manufacturing processes such as extrusion or injection molding occur at high shear rates, thereby the rheological properties of PP/MWCNT composites were measured on a high pressure capillary rheometer (Rheograph RG75, Göttfert, Germany) equipped with dies of 1 mm diameter and different lengths (30, 20 and 10 mm). The tests were performed over a range of temperatures (185 to 245°C) and shear rates (100 to 5000 s^{-1}) corresponding to various conditions. The PP/MWCNT pellets were dried under vacuum for 4 h at 80°C before testing.

The effective melt shear viscosity was determined using the corrected shear rate and shear stress based on the Weissenberg-Rabinowitsch correction (for non-parabolic velocity profile) and the linear Bagley correction (for pressure drop at the capillary entry), respectively.

* email: nicoleta.stanciu@ugal.ro

pVT Measurements

The pVT measurements were carried out using the Rheograph RG75 equipped with a pVT device. Dry pellets were loaded into the barrel with a diameter of 15 mm and pre-heated to 200°C. After loading at the maximum level of the barrel, a piston with a Teflon ring was inserted and the melt was extruded until about 18 mm of material was left in the barrel.

The pVT analysis is based on the isothermal compression in order of decreasing temperature from 220 to 90°C. For each temperature step, the pressure was scanned in increasing order from 10 to 1250 bar. It should be noted that between two consecutive temperatures the sample inside the barrel was kept under constant force of 5 kN, while before each measurement step, the material was allowed to relax for 10 minutes.

Results and discussions

Melt Shear Viscosity

Figure 1 presents the variation of melt shear viscosity as a function of shear rate for different MWCNT wt.% at two different temperatures (200 and 230°C). The apparent melt shear viscosity decreases with increasing shear rate and melt temperature. At higher shear rates (> 100 s^{-1}) all PP/MWCNT composites behave like a shear thinning fluid, with their melt shear viscosity linearly related to the apparent shear rate, as shown in figure 1. It should be noted that no flow instability occurred during the measurements, a smooth stream of PP/MWCNT composites being produced at the exit of the capillary die.

On the other hand, the melt shear viscosity increases with increasing nanotube wt.%. As the MWCNT loading increases, the number of nanotubes per unit volume which comes into contact during flow increases and the inter-particle interaction becomes stronger and thus the viscosity of the molten composite increases [29]. Moreover, CNTs can restrict the mobility of the polymer chains and thus increase of melt shear viscosity [12, 15].

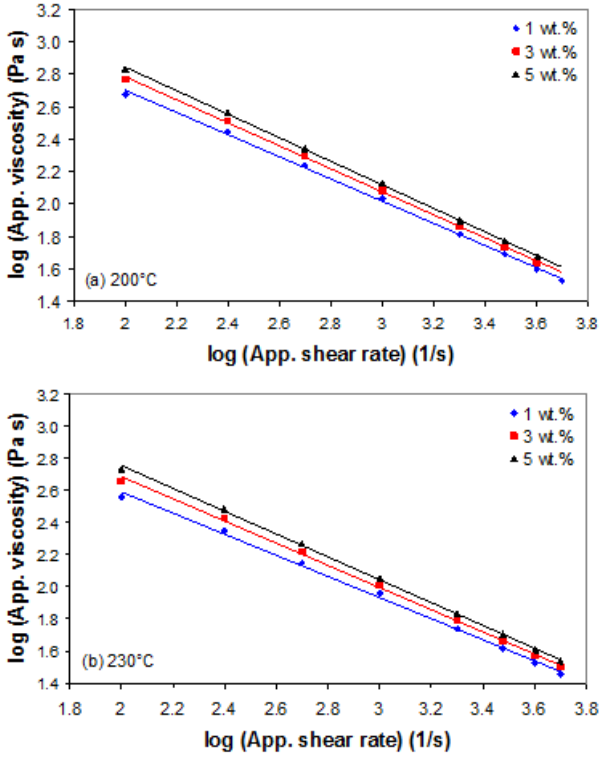

Fig. 1. Melt flow curves for PP/MWCNT composite at different melt temperatures

Figure 2 shows the temperature dependence of melt shear viscosity for two different apparent shear rates (500 and 1000 s^{-1}). In the temperature range of 185 to 245°C, the dependence of melt shear viscosity on the reciprocal absolute temperature ($1/T$) is linear, as shown in figure 2.

Since the melting temperature is well above T_t+100, the linear temperature-viscosity dependence in figure 2 can be used to estimate the flow activation energy. The solid line in figure 2 represents the best fit of experimental data with the Arrhenius equation [32, 33], and the slope of this line gives the apparent activation energy of flow. For the data presented in figure 2, the average slope (1048.35±76.35, 1060.65± 26.65 and 1126.35± 39.15 for PP/MWCNT melt composite with 5, 3 and 1 wt.%) slightly increases with decreasing nanotube wt.% and is practically independent of the shear rate.

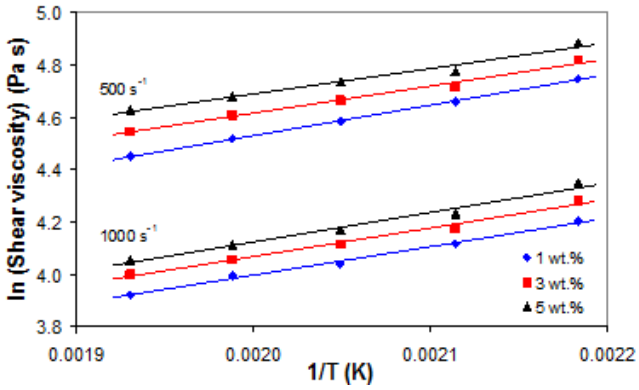

Fig. 2. Arrhenius plot for PP/MWCNT composites

Figure 3 presents the variation of apparent melt shear viscosity as a function of MWCNT wt.% for different shear rates at 200°C. A linear relationship was used to estimate the dependence of the melt shear viscosity on the MWCNT wt.%. As shown in table 1, both the slope and the intercept of the straight line decrease with increasing apparent shear rate, indicating that the sensitivity of PP/MWCNT composites is weakened with increasing apparent shear rate.

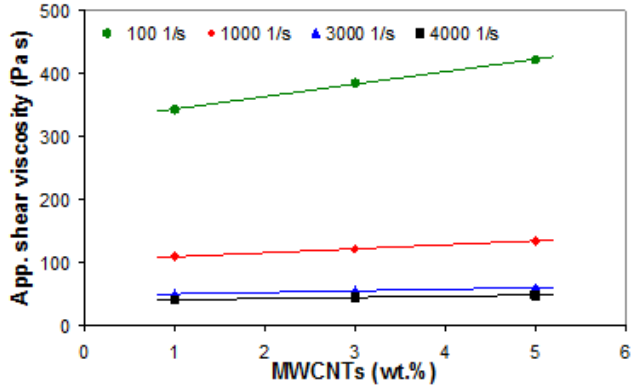

Fig. 3. Effect of nanotube wt.% on melt shear viscosity of PP/MWCNT composite at 200°C

Table 1

DEPENDENCE OF VISCOSITY ON MWCNT LOADING AT 200°C

App. shear rate (1/s)	Slope (Pa s/wt.%)	Intercept (Pa s)
100	19.865	323.6
1000	6.3754	101.81
3000	2.4826	46.50
4000	1.9126	37.69

Rheological modeling

From the shear viscosity vs. shear rate curves shown in figure 1, it is obvious that the rheological model, which relates the melt shear viscosity with the shear rate, should describe the flow for medium and high shear rate range. The problem which arises in simulation of the injection molding process is in the choice of rheological models for calculating the material parameters from the experimental values. When dealing with the simulation of the injection molding process, two models are popular, i.e. Cross model and Carreau-Winter model thereby these models will be considered in this study.

According to the 3-parametric Cross model, the melt shear viscosity at a give shear rate is given by [32-34].

$$\eta(\dot{\gamma}) = \frac{\eta_0}{1 + \left(\frac{\eta_0 \cdot \dot{\gamma}}{\tau^*}\right)^{1-n}} \quad (1)$$

where η_0 is the zero-shear rate viscosity, τ^* is the critical shear stress at which the onset of shear thinning behavior occurs, and n is the shear-thinning index.

The equation for the Carreau-Winter model is given as follows [33]

$$\eta(\dot{\gamma}) = \frac{\eta_0}{(1 + \lambda\dot{\gamma})^{m_c}}, \quad (2)$$

where λ is the characteristic time, i.e. the inverse of the shear rate at which the shear-thinning behavior begins, m_c is the viscosity exponent.

The Cross model usually is applicable in the medium to high shear rate domain, and has a problem with the prediction of zero-shear viscosity whereas the Carreau-Winter model is more appropriate in the low to medium shear rate domain [33].

Figure 4 illustrates the predicted values for the melt shear viscosity using the Cross model. The Cross model fits well the experimental data with a correlation coefficient $R^2 > 0.995$. The melt shear viscosity curves in figure 4 indicate

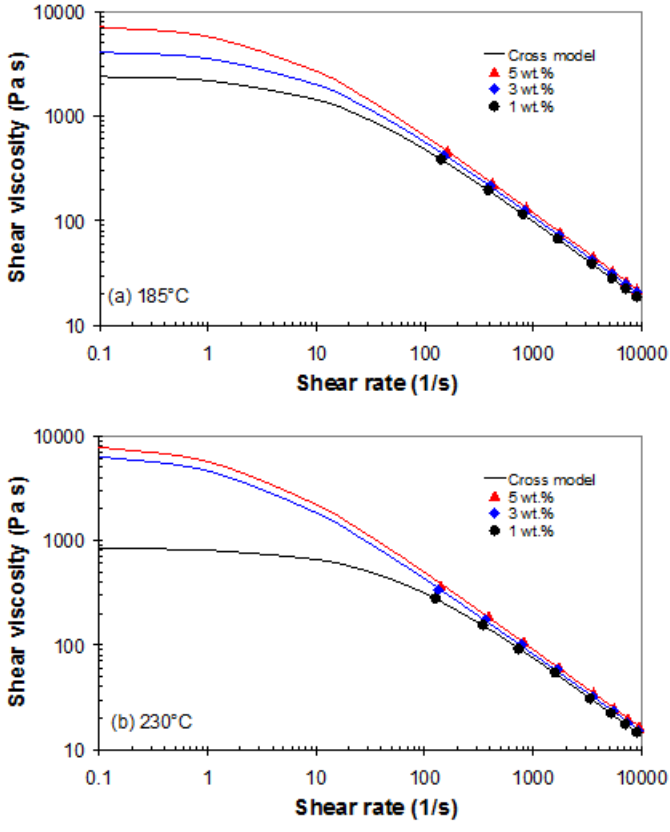

Fig. 4. Experimentally determined melt shear viscosity data and Cross model predictions for PP/MWCNT composites

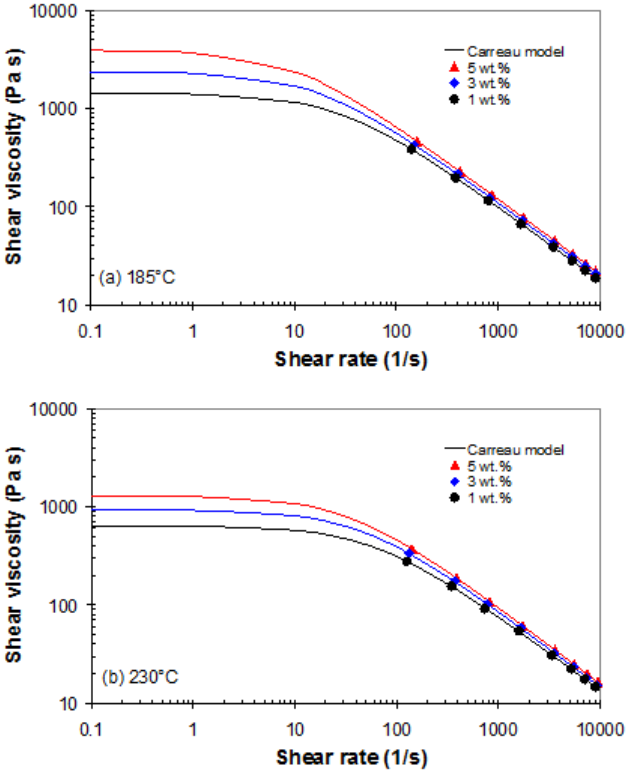

Fig. 5. Experimentally determined melt shear viscosity data and Carreau-Winter model predictions for PP/MWCNT composites

a very short primary Newtonian plateau and a well developed pseudo-plastic region. The zero-shear viscosity predicted by the Cross model should be interpreted as an apparent value since no measurements were carried out at shear rates below 100 s^{-1}.

Figure 5 shows the predicted values for the melt shear viscosity using the Carreau-Winter model. The Carreau-Winter model was also found to accurately describe the measured melt shear viscosity data ($R^2 > 0.995$). Three distinct regions along the viscosity curves were predicted for all PP/MWCNT composite melts, as shown in figur e5, i.e. a well-developed primary Newtonian plateau, a transition region and a shear-thinning zone.

Comparing the Cross and Carreau-Winter model predictions in figures 4 and 5, it can be concluded that, when trying to predict the melt shear viscosity at low shear rates, the Cross model over-predict the melt shear viscosity especially at higher nanotube loading.

For each MWCNT wt.%, a master curves was generated from the experimental data via time-temperature-superposition (TTS) principle and the Williams-Landel-Ferry (WLF) shift factor [32, 34], as shown in figure 6. The corresponding parameters for the Cross and Carreau-Winter models obtained using the master curve are summarized in table 2. Using these master curves, the melt shear viscosity can be predicted over a wide range of shear rates.

Data in table 2 show that the shear-thinning index n is practically constant for all three PP/MWCNT composite melts (average value of 0.227 ± 0.0071), while all the other parameters vary with nanotube loading. The shear-thinning index n indicates that the PP filled with 1, 3 and 5 wt.% of MWCNTs is suitable for injection molding. The Carreau-Winter model also predicts shear-thinning behavior of PP/MWCNT composite; the viscosity exponent parameter m_c

Model	Parameter	MWCNTs (wt.%)		
		1	3	5
Cross	η_0 (Pa·s)	1277.59	2321.19	2776.86
	τ^* (Pa)	3.75×10^4	3.63×10^4	4.15×10^4
	n	0.234	0.229	0.217
	E_a (kJ/mol)	42.27	41.86	43.61
Carreau-Winter	η_0 (Pa·s)	841.29	1453.41	1980.43
	λ (s)	0.021	0.037	0.047
	m_c	0.759	0.764	0.773

Table 2
MASTER CURVE PARAMETERS FOR PP/MWCNT COMPOSITES AT A REFERENCE TEMPERATURE OF 215°C

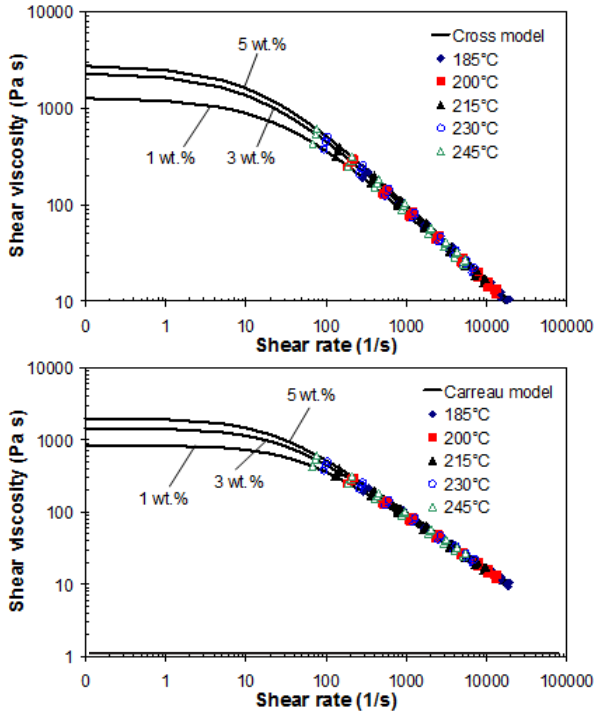

Fig. 6. Master viscosity curves for PP/ MWCNT composite from TTS principle at 215°C

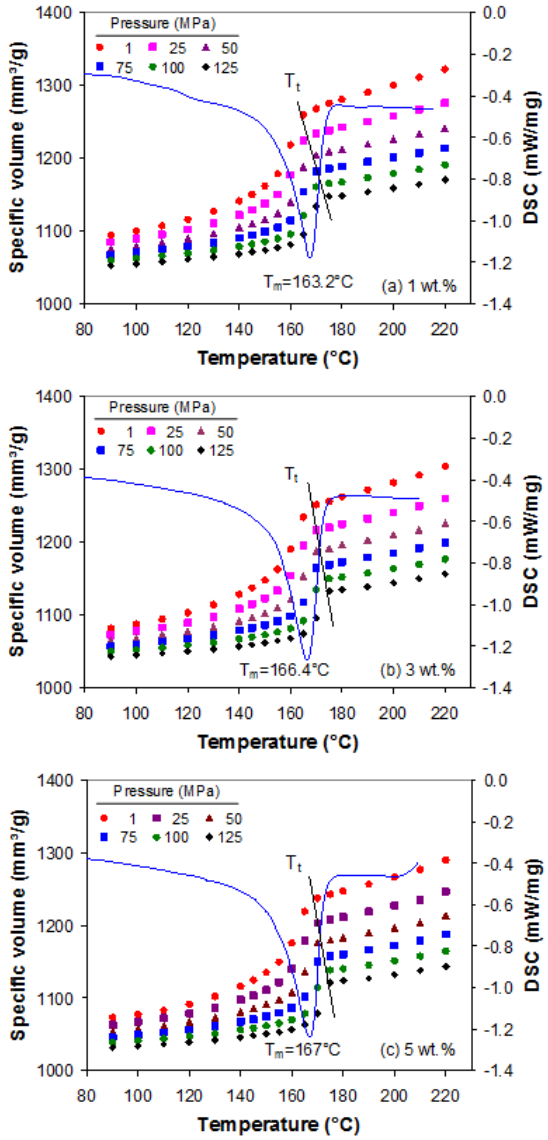

Fig. 7. pVT results and DSC for the PP/MWCNT composites

is practically independent of the nanotube loading (average value of 0.765 ± 0.0058).

The flow activation energy E_a of the PP/MWCNT melt composite via the Arrhenius equation is also presented in table 2. The E_a decreases marginally with increasing nanotube loadings up to 3 wt.%, and then increases with further increase of nanotube loadings. However, for non-Newtonian polymers the viscosity at fixed temperature is dependent on shear stress or shear rate. Therefore, constant shear rate activation energy may not be entirely correct [29]. Thus, the E_a values determined from the Arrhenius equation were compared to those obtained from the melt flow index (*MFI*) [11]. The advantage of using the *MFI* to determine the flow activation energy lies in the fact that *MFI* is measured at constant shear stress [29].

The activation energy of PP/MWCNT composite calculated from the *MFI* at 2.16 kg was found to be 43.67 kJ/mol for 1 wt.%, 46.5 kJ/mol for 3 wt.%, and 48.54 kJ/mol for 5 wt.% [11]. It can be seen that, for nanotube loading higher that 1 wt.%, the activation energy calculated from *MFI* is about 10% higher than that calculated from the Arrhenius equation. Thus, utilization of the Arrhenius equation for the determination of flow activation energy can be considered reasonable.

pressure-Volume-Temperature Data

The pVT data for the PP/MWCNT composite with 1, 3 and 5 wt.% are presented in figure 7. The first DSC melting scan is also shown in figure 7 [31]. The specific volume of the PP/MWCNT composite increases with increasing temperature and decreases with increasing pressure, the change in the solid state being much smaller than that in the molten state.

The pVT diagrams for the PP/MWCNT composite display three distinct zones: the melting zone, the transition zone, and the solid zone. As can be seen from figure 7, the transition zone shifted to higher value with increasing pressure (about 5 to 10°C).

Figure 8 shows the plot of the specific volume of the PP/MWCNT composite as a function of temperature and nanotube wt.% at p=50 MPa. The addition of nanotubes into the PP reduces the specific volume. This indicates that the dimensional stability of parts is improved because the carbon nanotubes limit the shrinkage of composite melt during cooling.

The experimental pVT data were fitted to the modified 2-domain Tait model [35]. According to this model, the relationship between the specific volume and the pressure and temperature is given by [35]:

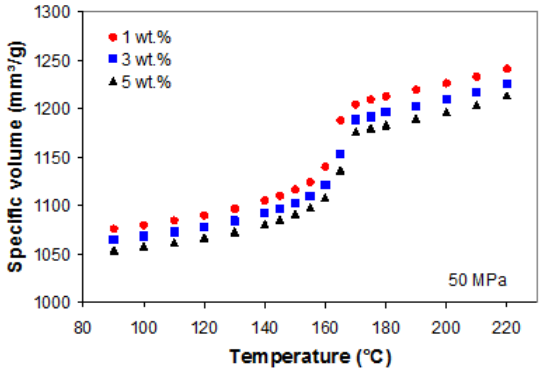

Fig. 8. pVT results for the PP/MWCNT composites at 50 MPa

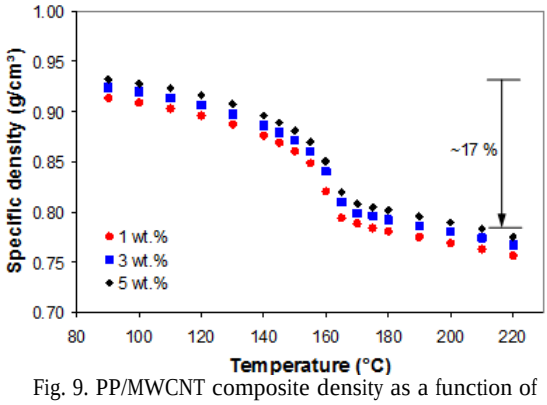

Fig. 9. PP/MWCNT composite density as a function of temperature at 1 MPa

$$V(T,p)=V_0(T)\cdot\left[1-C\cdot\ln\left(1+\frac{p}{B(T)}\right)\right]+V_t(T,p) \quad (3)$$

in which

$$V_0(T)=\begin{cases}b_{1s}+b_{2s}\cdot\tilde{T}, & T\le T_t;\\ b_{1m}+b_{2m}\cdot\tilde{T}, & T>T_t;\end{cases} \quad (4)$$

$$B(T)=\begin{cases}b_{3s}\cdot\exp(-b_{4s}\cdot\tilde{T}), & T\le T_t;\\ b_{3m}\cdot\exp(-b_{4m}\cdot\tilde{T}), & T>T_t;\end{cases} \quad (5)$$

$$V_t(T,p)=\begin{cases}b_7\cdot\exp(b_8\cdot\tilde{T}-b_9\cdot p), & T\le T_t\\ 0, & T>T_t\end{cases} \quad (6)$$

where: $\tilde{T}=T-b_5$, $T_t=b_5+b_6\cdot p$, b_1, b_1 to b_9 are model parameters.

Table 3
THE 2-DOMAIN TAIT PARAMETERS FOR PP/MWCNT COMPOSITE

Parameters	MWCNTs					
	1 wt.%		3 wt.%		5 wt.%	
	Melt	Solid	Melt	Solid	Melt	Solid
b_1 (mm³/g)	1264.53	1138.07	1249.95	1130.63	1235.72	114.24
b_2 (mm³/(g°C))	1.026	0.580	1.037	0.617	1.030	0.525
b_3 (bar)	580.55	1416.24	1570.93	1391.04	3151.99	1306.84
b_4 (1/°C)	0.00	7.10×10^{-3}	1.22×10^{-2}	8.09×10^{-3}	2.44×10^{-2}	7.68×10^{-3}
b_6 (°C/bar)	0.0075		0.0046		0.0046	
b_5 (°C)	164.481		168.778		168.779	
b_7 (mm³/g)	126.459		119.326		121.486	
b_8 (1/°C)	0.079		0.099		0.104	
b_9 (1/bar)	1.399×10^{-3}		1.051×10^{-3}		1.199×10^{-3}	

In the Tait model, the subscript *s* refers to solid state while *m* refers to melt state.

Fitting the experimental pVT data to the eq. 3 provides the parameters in the Tait model. All model parameters are given in table 3. The modified 2-domain Tait model provides a good fit to the measured pVT data. As can be seen the parameter $b_6 \neq 0$, confirming the effect of pressure on the transition temperature.

Specific Density

Figure 9 shows the change in density of PP/MWCNT composites with respect to temperature at 1 MPa pressure. All three composites present the same trend where density decreases with increasing temperature and increases with increasing nanotube wt.%. The density decreases by ~ 17% with increasing temperature from 90 to 220°C. The data in figure 9 can be used to estimate the melt density of PP/MWCNT composite, which also is a fundamental value for flow-simulation.

Conclusions

In this study, the effect of MWCNT wt.% and processing conditions (melt temperature, shear rate, and pressure) on the rheological behavior of polypropylene filled with 1, 3 and 5 wt.% of MWCNTs was investigated. A series of capillary rheological tests on PP/MWCNT composites were performed to determine the melt flow curves and pVT diagrams, and analytical models were fitted to the experimental data to extract the material parameters for simulation of manufacturing processes. Based on the experimental data, the following conclusions were formulated:

(i) The melt shear viscosity decreases with increasing melt temperature and shear rate, and increases with increasing MWCNT wt.%. All PP/MWCNT melt composites display shear-thinning behavior at high shear rates. The Cross and Carreau-Winter models provide a good fit to the experimental data in the medium to high shear rate range. At low shear rates, the Carreau-Winter model was found to better predict the melt shear viscosity.

(ii) At constant shear rate, the flow activation energy estimated from the Arrhenius equation slightly increases with increasing nanotube loadings, depending on the shear rates. Moreover, the flow activation energy from the Arrhenius equation is comparable with the flow activation energy from the melt flow index.

(iii) The specific volume of PP/MWCNT composite decreases with increasing MWCNT wt.% and pressure and increases with increasing temperature. The transition temperature was found to be pressure dependent. The 2-domain Tait model provides a good representation of the measured pVT data.

The findings in this study demonstrate that the addition of MWCNTs into the polypropylene matrix is feasible from melt processing point of view. Further research is needed to better understand how MWCNTs influence the melt shear viscosity at low shear rates.

Acknowledgments: This research was partially funded by the POSCCE Project P0102421/5117/22.05.2014 (COD SMIS 50414).

References

1.BREUER O., SUNDARARAJ U., Polym. Compos., **25**, nr. 6, 2004, p. 630;
2.COLEMAN J.N., KHAN U., BLAU W.J., GUNKO Y.K., Carbon, **44**, 2006, p. 1624;
3.ESAWI A.M.K., FARAG M.M., Mater. Des., **28**, 2007, p. 2394;
4.AL-SALEH M.H., SUNDARARAJ U., Composites Part A, **42**, 2011, p. 2126;
5.HAYASHI T., ENDO M., Composites Part B, **42**, 2011, p. 2151;
6.FERNANDEZ M., LANDA M., MUNOZ M.E., SANTAMARÍA A., Eur. Polym. J., **47**, nr. 11, 2011, p. 2078;
7.STAN F., FETECAU C., STANCIU N.V., ROSCULET R.T., SANDU I.L., ASME International Manufacturing Science and Engineering Conference, 2017;
8.ABBASI S., CARREAU P.J., DERDOURI A., Polymer, **51**, 2010, p. 922;
9.NARIMANI A., HEMMATI M., Polym Polym. Compos., **22**, nr. 6, 2013, p. 533;
10.LEE S.H., CHO E., JEON S.H., YOUN J.R., Carbon, **45**, 2007, p. 2810;
11. STAN F., SANDU I.L., FETECAU C., ASME International Manufacturing Science and Engineering Conference, 2015;
12. STAN F., FETECAU C., STANCIU N.V., Composites Part B, **110**, 2017, p. 20;
13. LI D., ZHAI T., GONG Q., FEI G., XIA H., Plast. Rubber Compos., **44**, nr. 5, 2015, p. 197;
14.GRACIA-FERNANDEZ C., GOMEZ-BARREIRO S., LOPEZ-BECEIRO J., NAYA S., ARTIAGA R., J. Therm. Anal. Calorim., **115**, nr. 2, 2014, p. 1727;
15.LIANG J.Z., et. al., Polym. Test., **45**, 2015, p. 41;
16.PALZA H., REZNIK B., KAPPES M., HENNRICH F., NAUE I. F. C., WILHELM M., Polymer, **51**, nr. 16, 2010, p. 3753;
17.McNALLY T., POTSCHKE P., A volume in Woodhead Publishing Series in Composites Science and Engineering, 2011, ISBN: 978-1-84569-761-7;
18.SHAFFER M.S.P., Windle A.H., Adv. Mater., **11**, 1999, p. 937;
19.RODRIGUEZ E., FERNANDEZ M., MUNOZ M.E., SANTAMARIA A., J. Rheol., **60**, nr. 6, 2016, p. 1199;
20.WALSH D., ZOLLER P., J. Polym. Sci., Part A: Polym. Chem., **34**, nr. 7, 1996, p. 1365.
21.TAO R., SIMON S.L., J. Polym. Sci., Part B: Polym. Phys., **53**, nr. 16, 2015, p. 1131;
22.WANG J., 2012, ISBN: 978-953-51-0297-7;
23.UTRACKI L.A., SIMHA R., GARCIA-REJON A., Macromolecules, **36**, nr. 6, 2003, p. 2114;
24.UTRACKI L.A., SIMHA R., Macromolecules, **37**, 2004, p. 10123;
25.SPERANZA V., VIETRI U., Pantani R., Macromol. Res., **19**, nr. 6, 2011, p. 542;
26.YAMASAKI S., NISHIGUCHI D., KOJIO K., FURUKAWA M., Polymer, **48**, nr. 16, 2007, p. 4793;
27.WANG M., FAN X., THITSARTARN W., HE C., Polymer, **58**, 2015, p. 43;
28.RUEDA M.M., AUSCHER M.-C., FULCHIRON R., PERIEC T., MARTIN G., SONNTAG P., CASSAGNAU P., Prog. Polym. Sci., **66**, 2017, p. 22;
29.SHENOY A.V., Springer Netherlands, 1999;
30.*** Nanocyl Technical Data Sheet, www.nanocyl.com
31.STAN F., SANDU I.L., FETECAU C., Composites Part B, **59**, 2014, p. 109;
32.MORRISON F.A., Oxford University Press, 2001;
33.*** Program documentation: WinRheo II, Gottfert.
34.LIMA P., MAGALHAES DA SILVA S.P., OLIVEIRA J., COSTA V., Polym. Test., **45**, 2015, p. 58;
35.CHANG R.Y., CHEN C.H., SU K.S., Polym.

Manuscript received: 15.09.2018